This full text paper was peer reviewed at the direction of IEEE Communications Society subject matter experts for publication in the WCNC 2010 proceedings.

Interference Modeling for Cognitive Radio Networks with Power or Contention Control

Zengmao Chen[1], Cheng-Xiang Wang[1], Xuemin Hong[1], John Thompson[2], Sergiy A. Vorobyov[3], and Xiaohu Ge[4]
[1]Joint Research Institute for Signal and Image Processing, Heriot-Watt University, Edinburgh, EH14 4AS, UK.
[2]Joint Research Institute for Signal and Image Processing, University of Edinburgh, Edinburgh, EH9 3JL, UK.
[3]Department of Electrical and Computer Engineering, University of Alberta, Edmonton, AB, T6G 2V4, Canada.
[4]Department of Electronics and Information Engineering, Huazhong University of Science and Technology, Hangzhou, China.
Email: {zc34, cheng-xiang.wang, x.hong}@hw.ac.uk, john.thompson@ed.ac.uk, vorobyov@ece.ualberta.ca, xhge@mail.hust.edu.cn

***Abstract*—In this paper, we present an interference model for cognitive radio (CR) networks employing power control or contention control scheme. The probability density functions (PDFs) of the interference received at a primary receiver from a CR network are derived for two cases. For the first case, a power control scheme is proposed to govern the transmission power of a CR node. For the second one, a cognitive media access control (MAC) employs carrier sense multiple access with collision avoidance (CSMA/CA) based contention control to coordinate the operation of CR nodes with transmission requests. These two control schemes are compared in terms of their resulting interference distributions. It is demonstrated that both power and contention controls are effective approaches to alleviate the interference caused by CR networks. Some in-depth analysis for the impact of key parameters on the interference of CR networks is given via numerical studies as well.**

***Index Terms* – cognitive radio, interference modeling, power control, contention control.**

I. Introduction

With the desirable merit to improve spectrum utilization significantly, the newly emerged CR technology [1]– [3] has attracted more and more attention. A CR network is envisioned to be capable of reusing the unused or underutilized spectra of incumbent systems (also known as primary networks) by sensing its surrounding environment and adapting its operational parameters autonomously. One of the fundamental premises of a CR network is that it must not impose detrimental interference to the incumbent network. Therefore, modeling and analyzing the interference caused by CR networks is of great importance to reveal how the service of a primary network is deteriorated and how to deploy CR networks.

In the literature, the existing research on interference modeling for CR networks mainly falls into two categories: spatial and accumulated interference modeling. For spatial interference modeling, the fraction of white spaces available for CR networks was investigated in [4] and [5]. In [6], the region of interference for CR receivers and region of communication for CR transmitters were studied for the case where a CR network coexists with a cellular network. The interference from CR devices to wireless microphones operating in TV bands was analyzed in [7], where the operational area loss, i.e., the loss of reliable communication area, of a wireless microphone due to the existence of CR devices was examined. Besides spatial interference modeling, interference in the frequency domain was also researched in the literature, e.g., the interference due to out-of-band emission of a wireless regional area network (WRAN) was analyzed in [8].

As for accumulated interference modeling, in [9] the aggregate interference power from a sea of CR transmitters surrounding a primary receiver was derived. Also, the accumulated CR transmission power perceived at a primary receiver was given by integrating over the "CR sea" with a certain power density. The performance of a primary system was evaluated in [10] in terms of outage probability caused by the interference from CR networks. The outage probability was derived for the cases of both underlay and overlay spectrum sharing. In [11] the accumulated interference from multiple CR transmitters following a Poisson point process was approximated by a Gamma distribution and the probability of a primary receiver to be interfered was also given. It is worth noting that only path loss was assumed for the interfering channel in [9]–[11]. Their work was extended by taking both shadowing and fading into account in [12] and [13]. The PDF for accumulated interference and outage probability due to the aggregate interference from CR nodes were also derived in [12] and [13], respectively.

However, in all the previous works [4]– [13], CR transmitters were assumed to transmit at a fixed power level, i.e., no power control for CR transmitters was considered. Moreover, CR nodes were all assumed to communicate with each other simultaneously, which means that the cognitive MAC did not employ any contention control scheme. This paper focuses on aggregate interference modeling and aims at filling these research gaps by modeling interference from a CR network to a primary network accounting for control and contention control schemes. The PDFs of interference perceived at a primary network from a CR network are derived for either power or contention control. The impact of several key parameters on the resulting interference is evaluated as well for these two control schemes, which provides some insights for the deployment of CR networks.

The remainder of this paper is organized as follows. The system model is given in Section II. The detailed interference modeling is presented in Section III. The impact of several key parameters on the interference is analyzed via numerical

978-1-4244-6398-5/10/$26.00 ©2010 IEEE

studies in Section IV. Finally, we conclude the paper in Section V.

II. System Model

The system model is demonstrated in Figs. 1 and 2. Consider a CR network coexisting with a primary transmitter-receiver pair. The CR transmitters are distributed in a 2-dimension plane outside the *interference region* (IR) of the primary receiver as shown in Figs. 1 and 2. The IR is a disk centers at the primary receiver with radius R. It forbids any CR transmission within this circular region to protect the primary receiver against co-channel interference from the surrounding CR transmitters. Assume that all the CR transmitters reside in the same frequency spectrum as the primary transmitter and their transmissions are synchronized (the transmission for each CR node begins or ends at the same time). We aim at investigating the characteristics of interference perceived at the primary receiver.

The underlying interference channels from CR transmitters to the primary receiver experience pathloss, shadowing and fading. We express the pathloss function $g(r_j)$ as

$$g(r_j) = r_j^{-\beta} \tag{1}$$

where r_j is the distance from the jth active CR transmitter to the primary receiver ($j = 1, 2, \cdots$) and β is the pathloss exponent. The composite model for shadowing and fading can be expressed as the product of the short term multipath fading and the long term shadowing. Let h_j denotes the channel gain for the composite shadowing and fading of the interference channel from the jth active CR transmitter to the primary receiver. In this paper, the log-normal shadowing and the Nakagami fading are considered. The PDF for the composite channel gain h_j can be approximated as the following log-normal distribution [14]

$$f_h(x) \approx \frac{10}{\ln 10\sqrt{2\pi}\sigma x}\exp\left\{-\frac{(10\log_{10}x-\mu)^2}{2\sigma^2}\right\} \tag{2}$$

The mean μ and variance σ^2 in (2) can be expressed as [14]

$$\mu = \xi^{-1}\left(\sum_{k=1}^{m-1}\frac{1}{k} - \ln(m) - 0.5772\right) + \mu_\Omega \text{ [dB]} \tag{3}$$

$$\sigma^2 = \sum_{k=0}^{\infty}\frac{\xi^{-2}}{(m+k)^2} + \sigma_\Omega^2 \text{ [dB]} \tag{4}$$

where $\xi = (\ln 10)/10$, m is the Nakagami shape factor, μ_Ω and σ_Ω^2 are the standard mean and variance of the log-normal distribution.

Let p_j denote the transmission power of the jth active CR transmitter. The accumulated power of the instantaneous interference received at the primary receiver can be formulated as follows:

$$Y = \sum_{j=1}^{\infty} p_j g(r_j) h_j. \tag{5}$$

In this paper, we investigate the characteristics of the accumulated interference from all CR transmitters employing the following two different schemes, i.e., power control or contention control.

A. Power Control

In this scenario, as shown in Fig. 1 the distribution of active CR transmitters follows a Poisson point process with density parameter λ, which stands for the density of CR transmitters on the plane.

We assume that the transmission power of a CR transmitter is governed by the following power control law

$$p(r_{cc_j}) = \begin{cases} r_{cc_j}^{\alpha} & 0 < r_{cc_j} \le P_{\max}^{\frac{1}{\alpha}} \\ P_{\max} & r_{cc_j} > P_{\max}^{\frac{1}{\alpha}} \end{cases} \tag{6}$$

where α is the power control exponent, $P_{\max}$ is the maximum transmission power for CR transmitters, and r_{cc_j} is the distance from the jth CR transmitter to its nearest active CR transmitter. When CR transmitters follow a Poisson point distribution with density λ, the PDF of $\{r_{cc_j}\}$ can be given as [16]

$$f_{cc}(x) = 2\pi\lambda x \exp(-\lambda\pi x^2). \tag{7}$$

The above proposed power control scheme can guarantee that for the jth CR transmitter the interference caused by its nearest CR transmitter is $p(r_{cc_j})g(r_{cc_j})$, which is not larger than a constant when the power control exponent α in (6) equals the pathloss exponent β in (1). In other words, at any CR transmitter its interference from the nearest neighboring CR transmitter is capped and independent of their distance.

B. Contention Control

Unlike the previous power control scheme, for the case of contention control every active CR transmitter has fixed transmission power p, but their transmission is governed by contention control to determine which CR transmitters can transmit at a given time. We assume that the multiple access protocol CSMA/CA is employed, like in IEEE 802.11 networks. Every CR transmitter senses the medium before transmission. If the medium is busy, namely, the CR transmitter detects transmission from other CR transmitters within its contention region, it defers its transmission. Otherwise, the CR transmitter starts its transmission after a pre-determined random time. As the result of the contention control as shown in Fig. 2, all the active CR transmitters are separated from each other by at least the contention distance, which is the minimum distance $d_{\min}$ between two concurrent transmitting CR transmitters.

The distribution of the active CR transmitters under the contention control can be modeled as a Matern-hardcore (MH) point process [15], which can be considered as a thinned process from a Poisson point process [16]. The thinning operation deletes some points from the original Poisson process under certain criteria. The MH process Φ_{mh} is the result of dependent thinning from a Poisson point process Φ, i.e., whether deleting or retaining a point depends on previous

deletion operations. The mathematical expression of the MH process is given by [16]

$$\Phi_{mh}=\{x \in \Phi : m(x) < m(y) \text{ for all } y \text{ in } \Phi \cap C(x, d_{\min})\}. \quad (8)$$

Each point x in the Poisson point process Φ is marked with a random value $m(x)$ uniformly distributed in (0,1). $C(x, d_{\min})$ is a disk centering at point x with radius $d_{\min}$. The *retaining probability* $p_{\rm mh}$ for the MH process, which is the probability of a point from a Poisson point process with density λ surviving the thinning process, is given by [16]

$$p_{\rm mh} = \frac{1 - e^{-\lambda \pi d_{\min}^2}}{\lambda \pi d_{\min}^2}. \quad (9)$$

III. Interference Modeling

We intent to model the accumulated interference at a primary receiver from CR transmitters employing either power or contention control introduced in Section II by finding their corresponding PDFs. We adopt the same methodology as used in [12] and [17] to derive the PDFs. First, the characteristic functions of the interference under different system models are derived. Then, the PDFs of the accumulated interference are obtained by performing inverse Fourier transform on their characteristic functions.

A. Power Control

When all the CR transmitters follow a Poisson point process distribution and employ the power control scheme proposed in (6), we can adopt similar methodology as in [12], [17], [18] and [19] and obtain the following characteristic function $\phi_Y(\omega)$ of the accumulated interference Y at a primary receiver from all CR transmitters

$$\phi_Y(\omega) = \exp\left(\lambda\pi \int_H f_h(h) \int_P f_p(p) T(\omega p h) dp\ dh\right) \quad (10)$$

where $f_p(\cdot)$ is the PDF for the transmission power $\{p(r_{cc_j})\}$ of a CR transmitter defined in (6) and

$$T(\omega p h) = R^2(1 - e^{i\omega g(R) p h}) + i\omega p h \int_0^{g(R)} [g^{-1}(t)]^2 e^{i\omega t p h} dt. \quad (11)$$

In (11), $g^{-1}(\cdot)$ denotes the inverse function of $g(\cdot)$ in (1). For the derivation of (10), the following fact is used: the distances from the jth CR transmitter to the primary receiver $\{r_j\}$ ($j = 1, 2, \cdots$) have independent and identical uniform distributions [17]. Their PDFs have the following form [17]

$$f_r(x) = \begin{cases} 2x/(l^2 - R^2) & R \le x \le l \\ 0 & \text{otherwise} \end{cases} \quad (12)$$

when CR transmitters distribute within an annular ring with inner radius R and outer radius l. Equation (10) can be rewritten as

$$\phi_Y(\omega) = \exp\left(\lambda\pi \int_H f_h(h) \int_{r_{cc}} f_{cc}(r) T(\omega p(r_{cc}) h) dr dh\right). \quad (13)$$

This is due to the fact that p in (10) is a function of r_{cc} as shown in (6), so the expectation of $T(\omega p h)$ over p equals that of $T(\omega p(r_{cc}) h)$ over r_{cc}, whose PDF is given in (7). Substituting (6) and (7) into (13), we have (19) at the top of page 4.

Finally, we obtain the PDF of the interference by performing the inverse Fourier transform on $\phi_Y(\omega)$ as

$$f_Y(y) = \frac{1}{2\pi} \int_{-\infty}^{+\infty} \phi_Y(\omega) e^{-2\pi i \omega y} d\omega. \quad (14)$$

Equations (13) and (14) serve as general expressions of the characteristic function and PDF, respectively, of the interference under the power control scheme. As a special case, when the pathloss exponent $\beta = 4$ and the radius of the interference region $R = 0$, the PDF $f_Y(y)$ can be further simplified as

$$f_Y(y) = \frac{\pi}{2} K \lambda y^{-3/2} \exp\left(-\frac{\pi^3 \lambda^2 K^2}{4y}\right) \quad (15)$$

where

$$\begin{aligned} K &= \int_H f_h(h) \int_P f_p(p) \sqrt{hp}\ dp dh \\ &= \int_H f_h(h) \sqrt{h}\ dh \int_P f_p(p) \sqrt{p}\ dp \\ &= \int_H f_h(h) \sqrt{h}\ dh \left(\int_0^{P_{\max}^{\frac{1}{\alpha}}} 2\pi\lambda e^{-\lambda\pi r^2} r^{\frac{\alpha}{2}+1} dr \right. \\ &\qquad \left. + \int_{P_{\max}^{\frac{1}{\alpha}}}^{\infty} 2\pi\lambda r e^{-\lambda\pi r^2} \sqrt{P_{\max}}\ dr \right). \end{aligned} \quad (16)$$

B. Contention Control

As mentioned in Section II-B, the distribution of CR transmitters can be modeled as a MH point process when the contention control is adopted. The MH process is a dependent thinning process from an original Poisson point process, which means that the position of each CR transmitter is correlated to each other. Therefore, it is very challenging to find a closed-form PDF as (12) to characterize the distance random variables $\{r_j\}$ in this scenario. Instead, we treat the MH point process as a thinned Poisson point process with retaining possibility $p_{\rm mh}$ given in (9). Then, the accumulated interference power perceived at the primary receiver can be express as

$$Y = \sum_{j=1}^{\infty} p_{\rm mh} p_j g(r_j) h_j. \quad (17)$$

This equation interprets the contention control scheme as follows: all the CR transmitters still follow Poisson point process with intensity λ, but the jth CR transmitter has possibility $p_{\rm mh}$ to transmit at power level p_j. Without loss of generality, we assume $p_j = 1$ W. Following the similar steps as in [12], the characteristic function of the accumulated interference can be written as

$$\phi_Y(\omega) = \exp\left(\lambda\pi \int_H f_h(h) T(\omega p_{\rm mh} h) dh\right) \quad (18)$$

$$\begin{aligned}\phi_Y(\omega) &= \exp\left\{\lambda\pi\int_H f_h(h)\int_{r_{cc}} f_{cc}(r)\Big(R^2\big(1-e^{i\omega g(R)p(r)h}\big)+i\omega p(r_{cc})h\int_0^{g(R)}\left(g^{-1}(t)\right)^2 e^{i\omega t p(r)h}dt\Big)dr\,dh\right\}\\ &= \exp\left\{\lambda\pi\int_H f_h(h)\int_0^{P_{\max}^{\frac{1}{\alpha}}} f_{cc}(r)\Big(R^2\big(1-e^{i\omega g(R)r^\alpha h}\big)+i\omega r^\alpha h\int_0^{g(R)}(g^{-1}(t))^2 e^{i\omega t r^\alpha h}dt\Big)dr\,dh\right.\\ &\quad\left.+\lambda\pi\int_H f_h(h)\int_{P_{\max}^{\frac{1}{\alpha}}}^{\infty} f_{cc}(r)\Big(R^2\big(1-e^{i\omega g(R)P_{\max}h}\big)+i\omega P_{\max}h\int_0^{g(R)}(g^{-1}(t))^2 e^{i\omega t P_{\max}h}dt\Big)dr\,dh\right\} \qquad (19)\\ &= \exp\left\{\lambda\pi\int_H f_h(h)\int_0^{P_{\max}^{\frac{1}{\alpha}}} 2\pi\lambda r\exp(-\lambda\pi r^2)\Big(R^2\big(1-e^{i\omega g(R)r^\alpha h}\big)+i\omega r^\alpha h\int_0^{g(R)}(g^{-1}(t))^2 e^{i\omega t r^\alpha h}dt\Big)dr\,dh\right.\\ &\quad\left.+\lambda\pi\int_H f_h(h)\int_{P_{\max}^{\frac{1}{\alpha}}}^{\infty} 2\pi\lambda r\exp(-\lambda\pi r^2)\Big(R^2\big(1-e^{i\omega g(R)P_{\max}h}\big)+i\omega P_{\max}h\int_0^{g(R)}(g^{-1}(t))^2 e^{i\omega t P_{\max}h}dt\Big)dr\,dh\right\}\end{aligned}$$

where

$$\begin{aligned}T(\omega p_{\rm mh}h) =& R^2(1-e^{i\omega g(R)p_{\rm mh}h})\\ &+i\omega p_{\rm mh}h\int_0^{g(R)}\left(g^{-1}(t)\right)^2 e^{i\omega t p_{\rm mh}h}dt. \quad (20)\end{aligned}$$

Similarily, its PDF can be obtained using (14). As a special case, when no IR is implemented and the pathloss exponent $\beta = 4$, the PDF can be simplified as

$$f_Y(y) = \frac{\pi}{2}K\lambda y^{-3/2}\exp\left(-\frac{\pi^3\lambda^2K^2}{4y}\right) \qquad (21)$$

where

$$K = \int_H f_h(h)\sqrt{p_{\rm mh}h}\;dh. \qquad (22)$$

So far, the PDFs of the interference received at a primary receiver from a CR network employing power control or contention control scheme have been derived, respectively. A natural extension of this work is to jointly consider both of these two control schemes, the detail of which is left for future work.

IV. Numerical Studies

The accumulated interference from CR transmitters employing power control or contention control is investigated via numerical studies in this section. For the power control scheme, Fig. 3 shows the PDFs of the accumulated interference with different power control exponents α and IRs. The detailed setup of this example scheme is as follows: the maximum transmission power for each CR transmitter $P_{\max} = 1$W, the density of CR transmitter $\lambda = 1$ user/10^4m^2, the pathloss exponent $\beta = 4$, the Nakagami shape factor $m = 1$, and the standard mean μ_Ω in (3) and variance σ_Ω^2 in (4) are 0 dB and 8 dB, respectivly. It can be seen from Fig. 3 that (i) both the mean and variance of the accumulated interference are significantly reduced when adopting the power control scheme; (ii) introducing IR also reduces the interference experienced at the primary receiver; (iii) increasing the power control exponent α leads to the decrease of interference. This is due to the fact that $r_{cc_j}^\alpha$ is a decresing function of α when $P_{\max} \le 1$W.

For the contention control scheme, we first confirm the correctness of derivations for the PDF of interference in Section III-B via a numerical simulation. In this experiment, we simulate a CR network with contention control and measure the PDF of the resulting interference. Then, this PDF is compared with the derived one. Fig. 4 shows this comparison. As we can see, there is a good agreement between the simulated and derived PDFs. It can also be seen from Fig. 4 that the simulated interference has slightly small mean and variance. This is due to the fact that in the derivation we assume infinite number of CR transmitters, while the number of CR transmitters is limited in the simulation, which means that we have fewer interferers in the simulation than in the derivation.

Fig. 5 depicts the PDFs of interference with different contention ranges $d_{\min}$ and IRs. It can be seen from Fig. 5 that (i) contention control greatly reduces both the mean and variance of the interference; (ii) similar to Fig. 3, introducing IR also reduces the interference received at the primary receiver.

The impact of CR transmitter density λ and contention range $d_{\min}$ is investigated in Fig. 6. Not surprisingly, it can been seen that the interference increases as λ increases and as $d_{\min}$ decreases. Fig. 6 also reveals another fact that the interference is more sensitive to the contention range compared to the CR transmitter density, e.g., in Fig. 6 the interference only increases slightly when doubling λ from 1 to 2 user/10^4m^2, while halving $d_{\min}$ from 160 to 80 m results in dramatic increase of interference. It means that manipulating the contention range is an effective approach to control the interference emitted to the primary receiver.

Finally, we study the impact of fading on the resulting interference with either power control or contention control in Figs. 7 and 8. From the comparison between Figs. 7 and 8, it can be seen that (i) shadowing and fading increase the variance of interference for both power control and contention control cases; (ii) the contention control scheme is more sensitive to shadowing and fading, since the variance of the interference increases more when experiencing shadowing and fading compared to the power control case.

V. Conclusions

In this paper, interference at a primary receiver caused by CR transmitters with either power control or contention control has been characterized. The PDFs of interference in these two cases have been evaluated numerically. Numerical studies have demonstrated that the proposed power control and contention control schemes are two effective approaches to alleviate interference caused by CR transmitters. Moreover, introducing IR can further protect a primary receiver against interfering CR transmitters. For the contention control scheme,

the impact of CR transmitter density and contention range on the interference has been analyzed. Finally, the influence of shadowing and fading on the interference with power control or contention control has been examined as well. Further work can be done to model interference from CR transmitters to a primary receiver when the knowledge of the primary receiver is imperfect.

ACKNOWLEDGMENTS

Zengmao Chen, Cheng-Xiang Wang, Xuemin Hong, and John Thompson acknowledge the support from the Scottish Funding Council for the Joint Research Institute in Signal and Image Processing between the University of Edinburgh and Heriot-Watt University which is a part of the Edinburgh Research Partnership in Engineering and Mathematics (ER-Pem). Sergiy A. Vorobyov acknowledges the support in part from the Natural Sciences and Engineering Research Council (NSERC) of Canada and in part from the Alberta Ingenuity Foundation, Alberta, Canada. Xiaohu Ge acknowledges the support from National Natural Science Foundation of China (NSFC) (contract/grant number: 60872007) and National 863 High Technology Program of China (contract/grant number: 2009AA01Z239). The authors acknowledge the support from the RCUK for the UK-China Science Bridges Project: R&D on (B)4G Wireless Mobile Communications.

REFERENCES

[1] S. Haykin, "Cognitive radio: brain-empowered wireless communications," *IEEE J. Sel. Areas Commun.*, vol. 23, no. 2, pp. 201–220, Sept. 2005.

[2] I. F. Akyildiz, W. Y. Lee, M. C. Vuran, and S. Mohanty, "NeXt generation/dynamic spectrum access/cognitive radio wireless networks: A survey," *Computer Networks*, vol. 50, no. 13, pp. 2127–2159, Sept. 2006.

[3] Q. Zhao and B. M. Sadler, "A survey of dynamic spectrum access," *IEEE Signal Process. Mag.*, vol. 24, no. 3, pp. 79–89, May 2007.

[4] X. Hong, C.-X. Wang, J. Thompson, and Y. Zhang,"Demystifying white spaces," *in Proc. IEEE ICCCAS'08*, Xiamen, China, May 2008, pp. 350-354.

[5] X. Hong, C.-X. Wang, H.-H. Chen, and Y. Zhang, "Secondary spectrum access networks: recent development on the spatial models," *IEEE Veh. Technol. Mag.*, vol. 4, no. 2, pp. 36-43, June 2009.

[6] T. Kamakaris, D. Kivanc-Tureli, and U. Tureli, "Interference model for cognitive coexistence in cellular systems," *in Proc. IEEE GLOBECOM'07*, Washington, DC, USA, Nov. 2007, pp. 4175–4179.

[7] R. S. Dhillon and T. X. Brown, "Models for analyzing cognitive radio interference to wireless microphones in TV bands," *in Proc. IEEE DySPAN'08*, Chicago, USA, Oct. 2008, pp. 1–10.

[8] G. L. Stuber, S. Almalfouh, and D. Sale, "Interference analysis of TV band whitespace," *in Proceedings of the IEEE*, vol. 97, no. 4, pp. 741-754, Apr. 2009.

[9] N. Hoven and A. Sahai,"Power scaling for cognitive radio," *in Proc. IEEE WNCMC'05*, Hawaii, USA, June 2005, pp. 250–255.

[10] R. Menon, R. M. Buehrer and J. Reed, "Outage probability based comparison of underlay and overlay spectrum sharing techniques," *in Proc. IEEE DySPAN'05*, Baltimore, USA, Nov. 2005, pp. 101–109.

[11] M. Timmers, S. Pollin, A. Dejonghe, A. Bahai, L. Van der Perre, and F. Catthoor, "Accumulative interference modeling for cognitive radios with distributed channel access," *in Proc. IEEE CrownCom'08*, Singapore, May 2008, pp. 1–7.

[12] X. Hong, C.-X. Wang, and J. S. Thompson, "Interference modeling of cognitive radio networks," *in Proc. IEEE VTC'08-Spring*, Singapore, May 2008, pp. 1851–1855.

[13] R. Menon, R. Buehrer, and J. Reed, "On the impact of dynamic spectrum sharing techniques on legacy radio systems," *IEEE Trans. Wireless Commun.*, vol. 7, no. 11, pp. 4198–4207, Nov. 2008.

[14] G. L. Stuber, *Principles of Mobile Communication*, 2nd Edition, Boston: Kluwer Academic Publishers, 2001.

[15] H. Q. Nguyen, F. Baccelli and D. Kofman, "A stochastic geometry analysis of dense IEEE 802.11 networks," *in Proc. IEEE INFOCOM'07*, Anchorage, USA, May 2007, pp. 1199-1207.

[16] D. Stoyan, W. S. Kendall, and J. Mecke, *Stochastic Geometry and Its Applications*, Chichester: John Wiley & Sons, 1986.

[17] E. S. Sousa and J. A. Silvester, "Optimum transmission range in a direct-sequence spread-spectrum multihop pack radio network," *IEEE J. Sel. Areas Commun.*, vol. 8, no. 5, pp 762–771, June 1990.

[18] X. Yang and A. P. Pertropulu, "Co-channel interference modeling and analysis in a Poisson field of interferers in wireless communications," *IEEE Trans. Signal Process.*, vol. 51, no. 1, pp. 63-76, Jan. 2003.

[19] P. C. Pinto and M. Z. Win, "Communication in a poisson field of interferers," *in Proc. IEEE 40th Annual Conf. Inform. Sciences and Systems*, Princeton, USA, Mar. 2006, pp. 432–437.

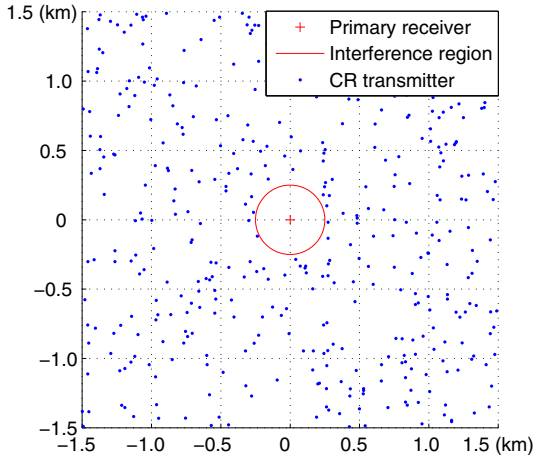

Fig. 1. System model for CR networks adopting power control ($R = 250$ m, and λ=0.5 user/10^4m^2).

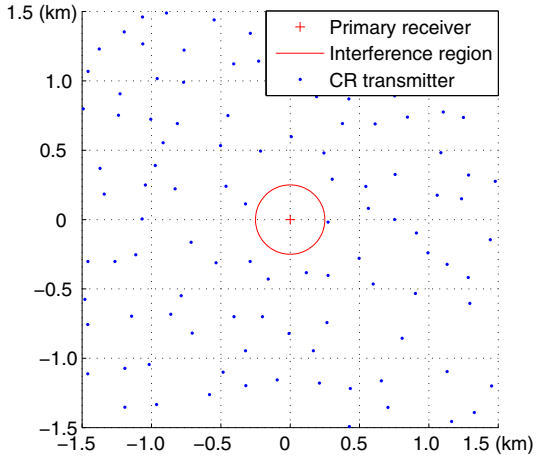

Fig. 2. System model for CR networks adopting contention control ($R = 250$ m, λ=0.5 user/10^4m^2, and $d_{\min}$=150 m).

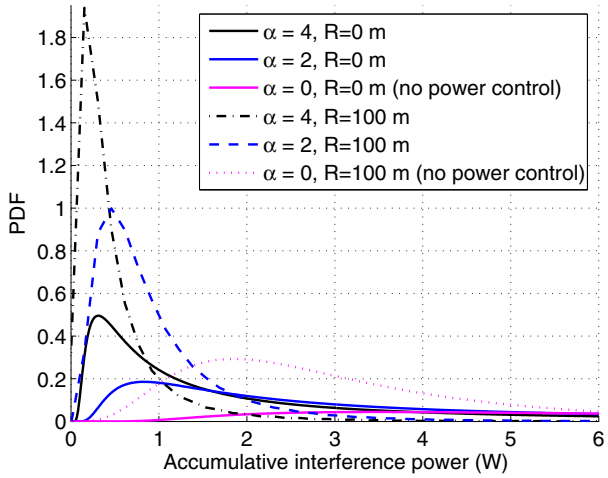

Fig. 3. Aggregated interference power PDFs with power control ($\lambda = 1$ user/10^4m^2, $P_{\max} = 1$ W, β =4, $m = 1$, and $\sigma_\Omega^2 = 8$ dB).

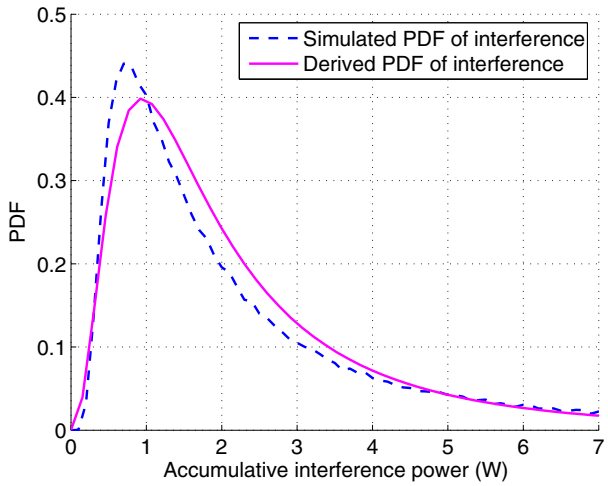

Fig. 4. Comparison between the derived and simulated interference PDFs for a CR newtork with contention control (R =100 m, λ =1 user/10^4m^2, β =4, m =1, and $\sigma_\Omega^2 = 8$ dB).

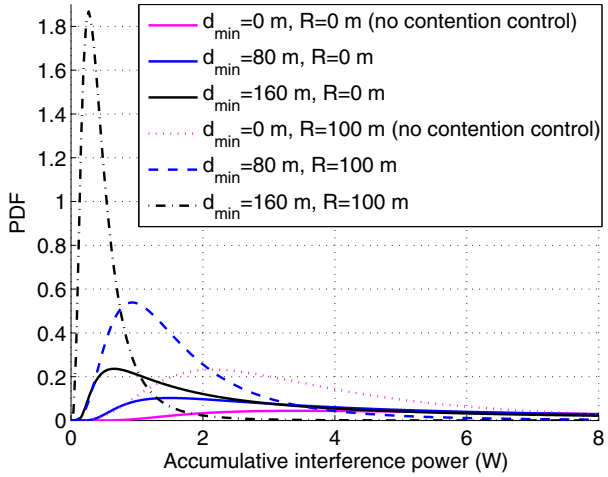

Fig. 5. Aggregated interference PDFs for a CR network with contention control ($\lambda = 1$ user/10^4m^2, β =4, $m = 1$, and $\sigma_\Omega^2 = 8$ dB).

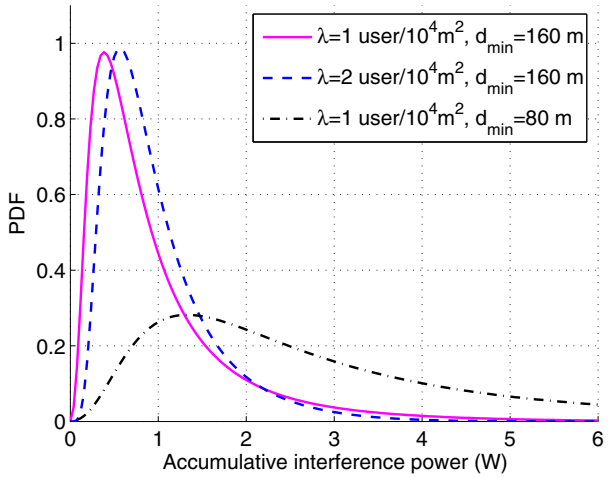

Fig. 6. Impact of CR user intensity and contention range on the aggregated interference for CR networks with contention control (R =100 m, β =4, $m = 1$, and $\sigma_\Omega^2 = 8$ dB).

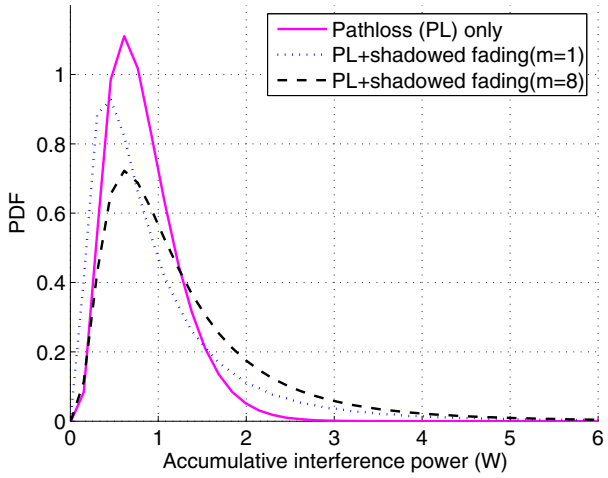

Fig. 7. Impact of fading on the aggregated interference for CR networks with power control (R =100 m, λ =1 user/10^4m^2, $P_{\max}$ =1 W, α =2, and σ_Ω^2 =8 dB).

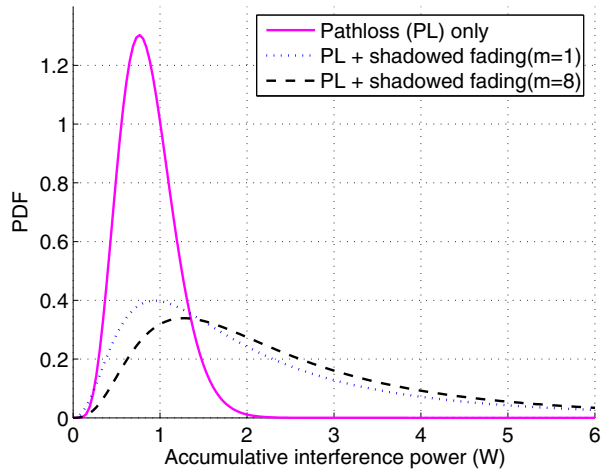

Fig. 8. Impact of fading on the aggregated interference for CR networks with contention control (R =100 m, λ =1 user/10^4m^2, $d_{\min}$ =100 m, and σ_Ω^2 =8 dB).